Aswan University Journal of Science and Technology Volume 3, issue 1, June 2023

# Numerical Prediction Of Bending Behavior Of Cold-Formed Steel Channels With Web Openings

Sedky Abdullah Tohamy*,[1], Khalid.FARAH[2], M.A.Saifeldeen[2], M. ABDELAZIM HASSAN[2,*]
[1]Department of civil Engineering, Minia University, Egypt
[2]Department of civil Engineering, Aswan University, Egypt

***ABSTRACT***

Cold-formed steel (CFS) sections are popular in structural and architectural applications because of their lightweight properties and high strength. To reduce floor height, different types of openings are added to the web of CFS beams, facilitating the passage of building services through the beams. This study aims to investigate the effectiveness of circular web openings in CFS beams using numerical simulations with finite element analysis (FEA) software (ABAQUS). Nonlinear three-dimensional finite element models (FEMs) for two CFS lipped channels were created and validated against experimental test results to determine failure mode and ultimate load-vertical displacement relationships. The models were then used to predict the bending behavior of CFS beams with circular web openings by varying the diameter and location of holes. The results showed that the load capacity of the beams decreased slightly when the ratio of hole diameter to web height ($d_w/h_w$) increased up to 0.5. However, there was a more significant decrease in load capacity when ($d_w/h_w$) ranged from 0.5 to 0.7.

**Keywords:** Cold-formed steel, Bending capacity, Local buckling, Finite Element Analyses, Openings

## 1. INTRODUCTION

Cold formed steel (CFS) Sections are commonly utilized as framing systems, floor joists, purlins, bracing, girts and shielding materials in building constructions. Introducing web holes in cold formed steel beams (CFSBs) is a common and important practice in structural buildings to let services like cables, piping, ducts and fire systems pass through openings of CFSBs, to minimize the floor height of these constructions. Although there are many shapes of web holes which can be used in CFSBs, the Circular openings are the most common shape of holes. The proper utilization of web holes can improve the architectural appeal and structural efficiency of CFSBs systems. So, studying the bending behavior of CFS channels with web openings is an important and necessary problem because of the significantly effect of these web opening on strength and failure characteristic of CFS members. In the recent decades, Studies on the structural behavior of CFSBs are increasingly popular because of their unique characteristics Such as, excessive slenderness, geometric imperfections and low torsional stiffness which are the primary factors that make CFSBs highly prone to buckling phenomena. Local buckling, distortional buckling, lateral-torsional buckling and their interactions, as shown in Figure (1), are the most complex and important problems within this research field [1-4]. Web openings studies in CFS members have been focused on the influence of these openings on the structural behavior of these members. However, most of these studies were focused on axial load capacity of CFS wall stud. A number of researchers had been succeeded to investigate the structural behavior including different failure modes and load capacities for many types of columns with web openings through conducting many of experimental and numerical studies [5-9]. On CFS channel columns with web openings, several experimental tests and finite element analyses (FEA) were conducted and direct strength method (DSM) was expanded to columns with web openings [10, 11]. In the recent year, the structural behavior of CFS channel beams with web openings has been investigated in many studies and reports. Many of FEA on edge stiffened web openings CFS channel beams were carried out to study the structural behaviors of these beams [12]. A number of nonlinear three-dimensional finite element models (FEMs) for built-up section consist of two CFS lipped channel beams face to face open sections and back-to-back closed sections with web holes has been carried out under two-point load to investigate the bending behavior and failure modes [13, 14]. Therefore, parametric studies in this paper are focused on the effectiveness of introducing different sizes of circular web openings diameter to mid span of cold formed channel beams under pure bending on moment capacities and different failure modes. According to construction guidelines of American Iron and Steel Institute (AISI)

Corresponding author E-mail: Mohamed.abdelazim@eng.aswu.edu.eg
Received April 5, 2023, received in revised form May 12, 2023, accepted May 19, 2023.
(ASWJST 2023/ printed ISSN: 2735-3087 and on-line ISSN: 2735-3095) https://journals.aswu.edu.eg/stjournal

[15], the ratio between openings diameter-to-web height ratio ($d_h/h_w$) doesn't exceed 70%. Numerical analysis was performed on CFS lipped channel beams with different sizes of circular web opening diameter under two-point load. The FEMs were verified against experimental tests results that available in the literature [16]. FE analysis results are presented in terms of the load deflection curves, failure modes, ultimate load capacities and showed the optimal range of openings diameter size for use.

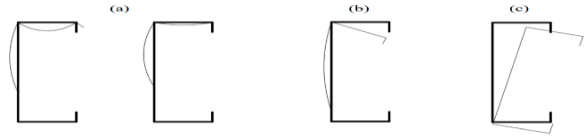


**Figure 1**: Lipped-channel beam (a) local, (b) distortional and (c) global (lateral-torsional) buckling modes.

## 2. EXPERMINTAL EVIDANCE

KS Sivakumaran, MY Ng and SR Fox [16] carried out a series of tests to study the structural behavior including the different failure modes and load capacities of CFS lipped channel beams with solid webs and beams with reinforced and unreinforced large single web openings at mid span. The test program was conducted on a wide range of CFS lipped channel beams divided into 11 groups of three identical. Test groups consist of channel specimen assembly with (1) solid webs; (2) regular standard industry web opening; (3) rectangular, square and circular web openings; (4) reinforced rectangular, square and circular web openings web openings and (5) another type of reinforced rectangular, square and circular web openings. The test specimens consisted of two monosymmetric CFS galvanized lipped channels with the same nominal depth 203.20 mm, nominal flange width 41.30 mm, nominal thickness 1.89 mm, inside bend radius 3.78 mm and the edge stiffener length 12.70 mm, as shown in Table (1). The total length of beam was 2743 mm, but the clear span was only 2543 mm. The test specimens were simply supported at their ends with one end hinged-supported and the other end roller-supported to allow for any horizontal movement under two equal point loads applying at the same distance from the supports, as shown in Figure (2). In order to investigate flexural behavior and establish the bending capacity, two lipped channel beams were used as test specimens to prevent lateral torsional buckling failure mode. So, the test specimen's flanges were fastened by steel brackets which work as a bearing plate at supports locations and loading points locations to prevent web crippling and lateral torsional buckling failure mode. Further, in the moment span between the loading points region, a 16 mm thick oriented strand board (OSB) was utilized lateral torsional restrains. In addition, lateral bracing consisted from a small strip of steel plate with 130 mm length, 20 mm width and 6.4 mm thick were fastened at the locations of supports and loading points to the nonbearing flanges to prevent lateral torsional buckling failure mode. Also, additional braces were attached to the compression flanges at the middle of shear span of the two beams of the specimen. The test results were given as failure modes and ultimate moment capacities and load-deflection curves as shown in Figure (3).

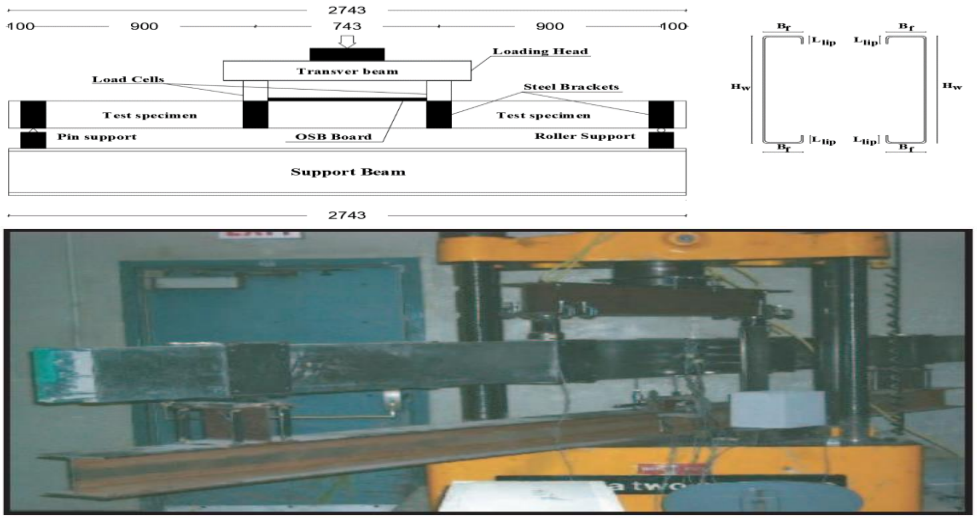


**Figure 2**: Experimental set-up for bending tests. All dimensions in millimeters [16].

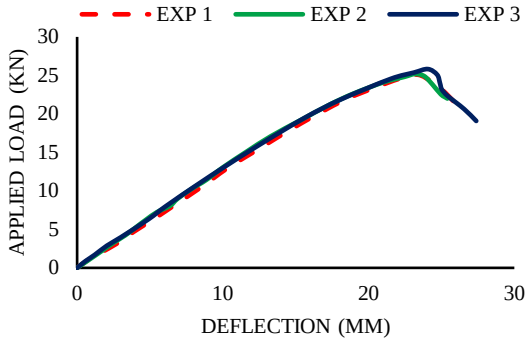


**Figure 3**: Experimental load-displacement relationships for channels with solid web [16].

## 3. NUMERICAL APPROACHES

### 3.1. Finite Element Model (FEM)

A series of nonlinear 3-D finite element models (FEMs) for simply supported lipped channel beams with and without web opening which allow for local buckling were developed by using finite element analysis software ABAQUS [17] to simulate two-point load test program as shown in Figure (1) which conducted by KS Sivakumaran, MY Ng and SR Fox [16]. A nonlinear numerical analysis was performed on FEM for CFS lipped channel beams with solid web to investigate the structural behavior of CFS test specimen. Also, another numerical analysis was performed on FEM for CFS lipped channel beam with single circular web opening at the mid span of beam with a diameter of 127 mm at the mid height of web of test specimen, as shown in Figure (4). It should be ensured that, local buckling mode is the FEM mode failure through applying appropriate boundary conditions to prevent lateral torsional buckling failure mode. FEA results gave a good agreement with an experimental result from comparing such results together in terms of ultimate load and failure modes and load-deflection relationships. The Dimensions of FEM cross section were obtained from Table (1) which gives the measured cross-section dimensions of test specimen as provided by KS Sivakumaran, MY Ng and SR Fox [16].

**Table 1**: Cross-section dimensions.

| | |
|---|---|
| Web height ($H_{web}$) | 203.20 mm |
| Flange width ($B_{flange}$) | 41.30 mm |
| Thickness (t) | 1.89 mm |
| Lip depth ($L_{lip}$) | 12.70 mm |
| Inside bend radius (r) | 3.78 mm |
| Length (L) | 2743 mm |
| Clear span (s) | 2543 mm |
| Shear span (a) | 900 mm |

#### 3.1.1. Element type

All CFSBs were simulated by using (S4R) general shell element reduced integration from ABAQUS software library [17] that considers shear transverse deformation as well as thick shell elements into simulation. In this Field, the shell element (S4R) was used by many researchers because of it decreased integration that reduced the necessary FEA time which CPU took to complete analysis.

#### 3.1.2. Material modeling

The material nonlinearity of the CFS was modelled using the Von-misses yield criteria with isotropic strain hardening. The stress-strain results of the coupon tests provided by KS Sivakumaran, MY Ng and SR Fox [16], as shown in Table (2). were utilized to define the material characteristics employed in numerical analysis. As shown in Figure (5), the behavior was specified as a quadrilinear curve. It should be observed that in this investigation, these material characteristics were applied to both the flat areas and the fillet corners of the sections. This is due to the possibility that some little changes in the numerical outputs when different properties of the material are included would be neglected.

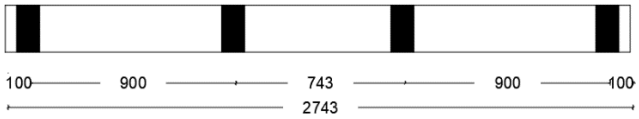


(a) Channel beam with solid web.

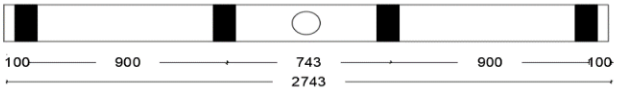


Channel Beam with mid-span circular web hole

Fig. 4. Proposed lipped channel beam section to FEA

3.1.3. Finite element mesh

At first, it was very essential to investigate the influence of the finite element mech size on the performance of CFSBs. Therefore, a numerical comparison conducted on three different mech sizes which were 5×5 mm (length by width), 10×10 mm and 20×20 mm. The three mech sizes provided good simulation results against experimental results. However, to complete analysis with 5×5 mm FE meshes size, it required a long time. On another hand, the accuracy which obtained from numerical analysis with 10×10 mm FE meshes size is better than results that obtained from 20×20 mm FE meshes size. So, in all simulations using the ABAQUS software in flat portion, FE meshes size of 10x10 mm (length by width) were chosen, to save time and get accurate results as shown in Figure (6). In the FE beam models, quadrangular shell element was utilized and it should be mentioned that around the circular web opening a smooth mesh transition was used.

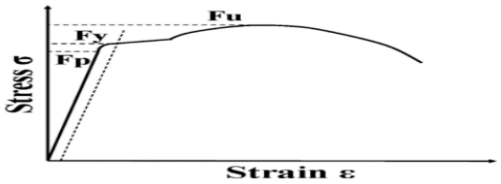


**Figure 5**: Stress-strain curve of the beam's steel [16].

Table 2: material properties of test beams [16]

| | |
|---|---|
| Proportional stress, $F_p$ (MPa) | 259 |
| Yield stress, $F_y$ (Mpa) | 324 |
| Ultimate stress, $F_U$ (Mpa) | 420 |
| $F_U/F_y$ | 1.30 |
| Rapture Strain, $\varepsilon_U$ (%) | 30 |

3.1.4. Loading and boundary conditions

The conducted loads and reactions forces were transferred from the load transfer beam which divided into two load cells to steel bracket and subsequently to the specimens during the beam testing. So, the interface between the steel brackets and the specimen was carefully simulated in the finite element model by using the coupling constraint, to restrain the surface motion to single point motion for each loading points and supports. The contact surfaces between the steel bracket and the specimen were defined as a surface set in each coupling constraint. A reference point was defined as a node set to simulate the loading points and support points. Lateral torsional buckling braces (steel plate strips & OSB) locations at the compression flanges were modeled as boundary conditions by constraining the translations and rotations of the brace locations at the top and bottom flange nodes in the x and approximately z-directions, respectively. The boundary conditions of simply supported were provided by releasing both the in-plane rotation and axial displacement along the beam at roller support. By using displacement control, the loads were provided in a static ricks step to the node sets at two load position of the beam with a defined value of displacement which must be more than the measured maximum deflection obtained from tests data to guarantee that FEA can complete the analysis up to the ultimate load.

## 4.VERIFICATION OF FINITE ELEMENT MODEL

The developed FEMs were validated with the published experimental results by KS Sivakumaran, MY Ng and SR Fox [16]. Firstly, for beam with solid web, The FEMs Load-deflection curve was verified against experimental results, as shown in Figure (7) and the mean value of the experimental-to-FEA load capacity ($P_{EXP}/P_{FEM}$) ratio was 1.04, as shown in Table (3) and the failure mode comparison for local buckling between the experimental and FEA results provided a good agreement, as shown in Figure (8). Second, for beam with single circular web opening, the FEMs Load-deflection curve was verified against Experimental results, as shown in Figure (9) and the mean value of the experimental-to-FEA load capacity ($P_{EXP}/P_{FEM}$) ratio was 1.05, As shown in Table (3) and the failure mode comparison for local buckling between the experimental and FEA results provided a good agreement, as shown in Figure (10). The comparisons of ultimate load and failure mode illustrate that the FEM accurately predicted the behavior of CFS beam under pure bending.

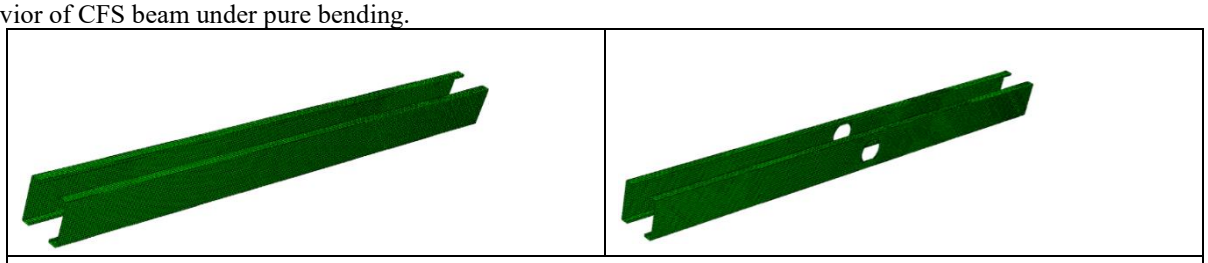

**Figure 6**: FE mech size 10×10 mm for beam with solid web and beam with circular web opening

**Table 3**: Ultimate Load capacities of Experimental and FEA beams.

| Beam | $P_{EXP}$ (KN) | $P_{FEM}$ (KN) | $P_{EXP}/P_{FEM}$ |
|---|---|---|---|
| Solid web | 25.50 | 25.40 | 1.04 |
| Web hole | 22.70 | 21.60 | 1.05 |

## 5. PARAMETRIC STUDY

After validation between Experimental and FEA results, it has been found that bending behavior and failure mode were accurately predicted by FEMs. So, Verified FEM was used to investigate the effect of web opening location with 127 mm diameter along the beam and the effect of diameter size on bending behavior of CFSBs with mid span single circular web opening. All FE analysis on CFSBs used Young's modulus E= $2.03 \times 10^5$ MPa, Yield stress $fy$= 259MPa and Poisson ratio ν=0.3 material properties. The ratio between hole diameter and web height ranged from 0.2 to 0.7 was used in parametric study. As Table (4) summarizes cross-section dimensions of CFSB, where web height is ($H_{web}$), flange width is ($B_{flange}$)

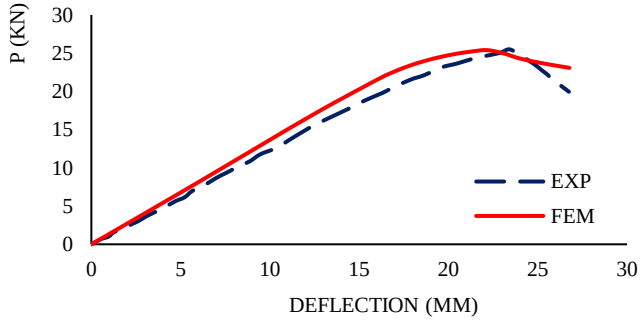


**Figure 7**: Comparison of load-displacement relationships obtained from experimental and FEA results for beam with solid web.

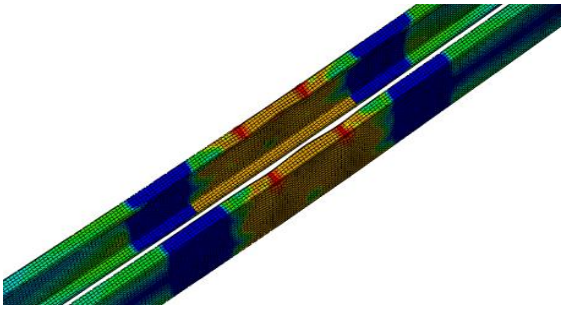

**Figure 8**: The experimental and FEA failure mode for Solid beam (C-r-0) [16].

and lip depth is ($L_{lip}$) and ratio between Hole diameter to web height is ($r = (d_h/h_w)$). For all sections the nominal thickness is 1.89 mm. The beams were labelled in such a way that identify the ratio between hole diameter to web height of beam. For example, a specimen labelled (C-r-0) refers to channel beam with solid web, whereas a specimen labelled (C-r-0.4) refers to channel beam with a web hole and the ratio between hole diameter size to web height is 0.4. The total length of FE beams was 2743mm with only 743 mm for moment span, as shown in Figure (4). Three cases were studied for the location of holes in addition to the case when the hole is located in the mid span of beam as shown in Figure (11).

## 6. RESULTS AND DISCUSSION

As illustrated in Figure (7), FEM produced a strong correlation of the load-deflection relationships for the solid beam (C-r-0) throughout the loading history. Furthermore, as shown in Figure (10), during the FE parametric studies, the numerical failure mode was close to the experimental failure mode, and it was shown that tested beams failed due to local buckling. This ensures that the parametric investigation provides accurate results. Results of FEMs with different hole diameter size to web height ratio (r) that ranged from 0.2 to 0.7, were compared together in term of load deflection curves, as shown in Figure (12). The Comparison illustrated that increasing the hole size to the fixed depth (r) leads to speed up the local buckling failure and reduce the value of load capacity. As shown in Figure (12), it is found that when the ratio between opening size and web depth increases up to 0.5, no significant effects on the load capacity of beams were found. However, when the ratio between opening size and web height increases from 0.5 to 0.7, there is an the obviously decreasing in load capacity. Table (4) shows maximum load values of FEMs for each beam and calculates the load reduction ratio in beams with web hole to beam with solid web which shown in Figure (13) and table (5) shows the maximum load values for cases of holes locations. Results of FEMs with different holes locations along beam, were compared together in term of load deflection curves, as shown in Figure (14).

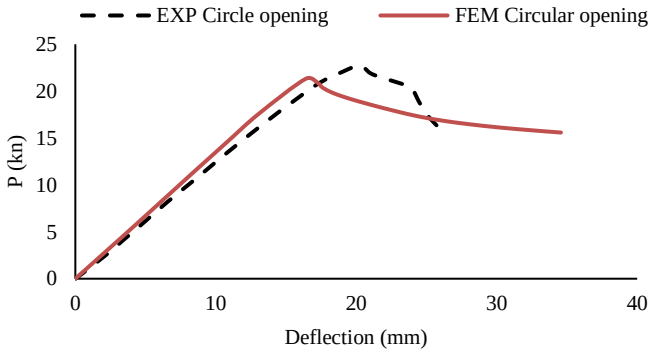


**Figure 9**: Comparison of load-displacement curves obtained from experimental and FEA results for beam with circular web opening

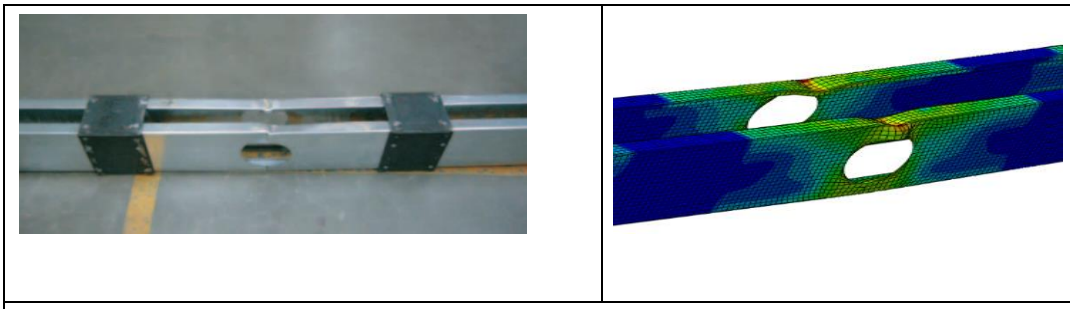

Fig. 10 The experimental and FEA failure mode for beam with circular web opening.[16]

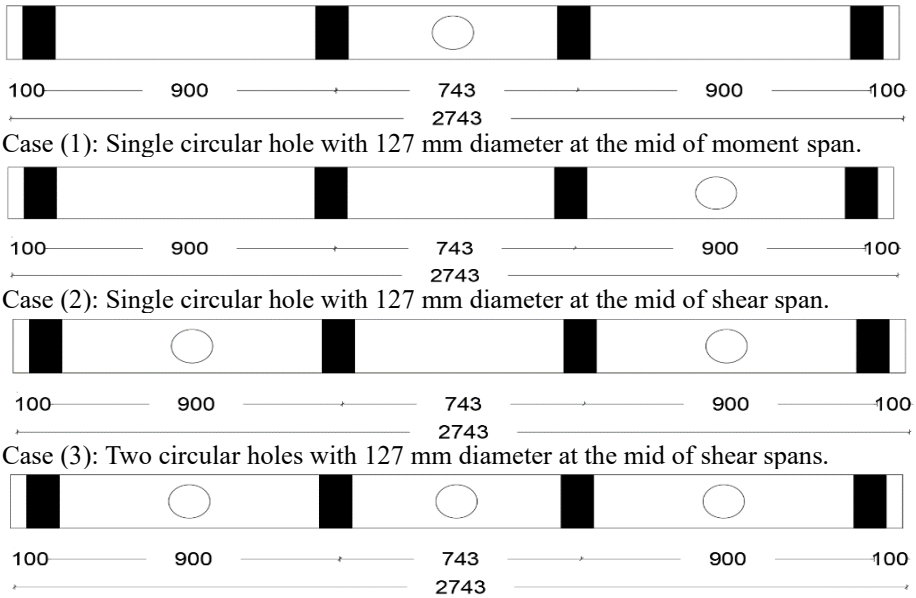


Case (1): Single circular hole with 127 mm diameter at the mid of moment span.

Case (2): Single circular hole with 127 mm diameter at the mid of shear span.

Case (3): Two circular holes with 127 mm diameter at the mid of shear spans.

Case (4): Three circular holes with 127 mm diameter at the mid of shear spans and the mid of moment span.

**Figure 11**: Cases of holes locations along CFS channel beam.

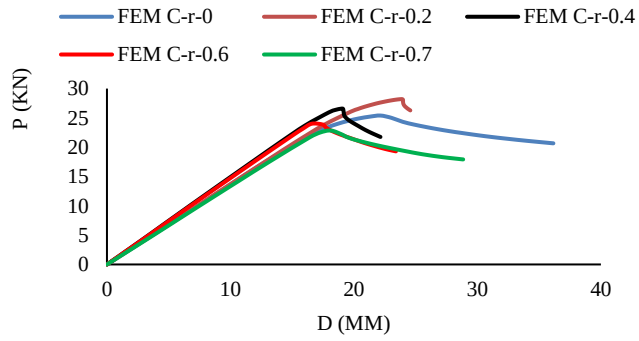


**Figure 12**: Comparison of load-displacement curves obtained from FEA results for beams with circular web opening

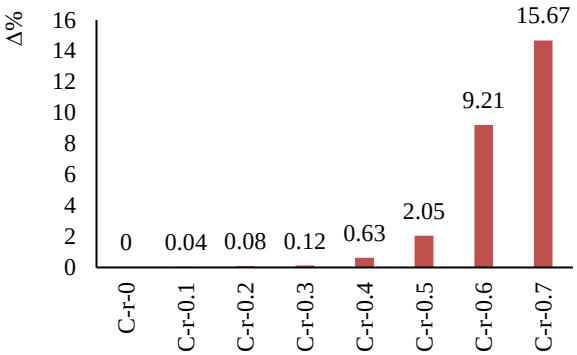


**Figure 13**: Load reduction curve for FE specimens.

**Table 4**: Max. load and cross-sections dimensions of FE beams.

| Sections | $h_w$ (mm) | $b_f$ (mm) | $l_p$ (mm) | d (mm) | $\frac{r}{d}$ ($\frac{d}{h_w}$) | Max. load $P_{FEM}$ | Δ% |
|---|---|---|---|---|---|---|---|
| C-r-0 | 203.20 | 41.30 | 12.70 | ---- | ---- | 25.40 | ---- |
| C-r-0.1 | 203.20 | 41.30 | 12.70 | 20.32 | 0.1 | 25.39 | 0.04 |
| C-r-0.2 | 203.20 | 41.30 | 12.70 | 40.64 | 0.2 | 25.38 | 0.08 |
| C-r-0.3 | 203.20 | 41.30 | 12.70 | 60.96 | 0.3 | 25.37 | 0.12 |
| C-r-0.4 | 203.20 | 41.30 | 12.70 | 81.28 | 0.4 | 25.24 | 0.63 |
| C-r-0.5 | 203.20 | 41.30 | 12.70 | 101.60 | 0.5 | 24.88 | 2.05 |
| C-r-0.6 | 203.20 | 41.30 | 12.70 | 121.92 | 0.6 | 23.06 | 9.21 |
| C-r-0.7 | 203.20 | 41.30 | 12.70 | 142.24 | 0.7 | 21.42 | 15.67 |

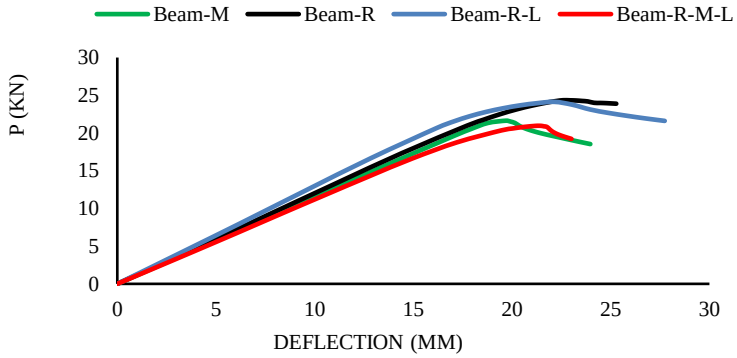


**Figure 14**: Comparison of load-displacement curves obtained from FEA results for web circular holes locations cases.

## 7. CONCLUSIONS

Holes must be inserted into web of the CFSBs during the manufacturing process in order to minimize clear height of the floor. Therefore, investigation of the effect of web hole diameter size on flexural behavior of CFSBs became a crucial problem. Test results including failure modes and load capacity of CFSBs with circular web openings were verified against numerical analysis results which were provided by FEA software ABAQUS. FEMs Results agreed well with experimental results. Based on the verified model, extensive parametric analyses on CFSBs with mid span single circular web hole were carry out. From these investigations can draw the following conclusions. CFSB failure is often caused by the excessive slenderness of CFS members. Geometric failure may happen before the section yields. So, introducing holes into the web leads to reduce load capacity and Precipitate local buckling failure. The effectiveness of web hole size on load capacity of CFSBs is relatively small when the ratio between the hole diameter to web height

increases up to 0.50 with a maximum load reduction about 3%. However, when the ratio between the hole diameter to web height increases from 0.50 to 0.70, the load capacity reduced obviously with a maximum load reduction about 16%. Hence, introducing circular web holes is recommended when the ratio between hole diameter size and web height doesn't exceed 50%, but if this ratio increases than 50%, beams should be strengthened to enhance moment capacity.

**REFERENCES**

[1] Yu, C. and Schafer, B. W. Local buckling tests on cold-formed steel beams. Journal of Structural Engineering-Asce, 129, 12 (Dec 2003), 1596-1606.
[2] Yu, C. and Schafer, B. W. Simulation of cold-formed steel beams in local and distortional buckling with applications to the direct strength method. Journal of Constructional Steel Research, 63, 5 (May 2007), 581-590.
[3] Wang, H. M. and Zhang, Y. C. Experimental and numerical investigation on cold-formed steel C-section flexural members. Journal of Constructional Steel Research, 65, 5 (May 2009), 1225-1235.
[4] Dinis, P. B. and Camotim, D. Local/distortional mode interaction in cold-formed steel lipped channel beams. Thin-Walled Structures, 48, 10-11 (Oct-Nov 2010), 771-785.
[5] Shanmugam, N. E. and Dhanalakshmi, M. Design for openings in cold-formed steel channel stub columns. Thin-Walled Structures, 39, 12 (Dec 2001), 961-981.
[6] Ritchie, D. and Rhodes, J. COLD-FORMED STEEL MEMBERS WITH PERFORATED ELEMENTS. Journal of the Structural Division-Asce, 100, NST9 (1974), 1960-1961.
[7] Loov, R. LOCAL BUCKLING CAPACITY OF C-SHAPED COLD-FORMED STEEL SECTIONS WITH PUNCHED WEBS. Canadian Journal of Civil Engineering, 11, 1 (1984), 1-7.
[8] Shanmugam, N. E., Thevendran, V. and Tan, Y. H. Design formula for axially compressed perforated plates. Thin-Walled Structures, 34, 1 (May 1999), 1-20.
[9] Ortiz-Colberg, R. A. The load carrying capacity of perforated cold-formed steel columns. Cornell University, Aug., 1981.
[10] Moen, C. D. and Schafer, B. W. Experiments on cold-formed steel columns with holes. Thin-Walled Structures, 46, 10 (Oct 2008), 1164-1182.
[11] Moen, C. D. and Schafer, B. W. Direct Strength Method for Design of Cold-Formed Steel Columns with Holes. Journal of Structural Engineering-Asce, 137, 5 (May 2011), 559-570.
[12] Yu, C. Cold-formed steel flexural member with edge stiffened holes: Behavior, optimization, and design. Journal of Constructional Steel Research, 71 (2012), 210-218.
[13] Wang, L. P. and Young, B. Beam tests of cold-formed steel built-up sections with web perforations. Journal of Constructional Steel Research, 115 (Dec 2015), 18-33.
[14] Wang, L. P. and Young, B. Design of cold-formed steel built-up sections with web perforations subjected to bending. Thin-Walled Structures, 120 (Nov 2017), 458-469.
[15] iron, A., specifications, s. i. C. o., members, C. s. a. T. c. o. c. f. s. s. and acero, M. C. n. d. l. i. d. h. y. d. North American specification for the design of cold-formed steel structural members. American Iron and Steel Institute, 2001.
[16] Sivakumaran, K. S., Ng, M. Y. and Fox, S. R. Flexural strength of cold-formed steel joists with reinforced web openings. Canadian Journal of Civil Engineering, 33, 9 (Sep 2006), 1195-1208.
[17] Abaqus Users Manual, Version 6.14-1, Dassault Systèmes Simulia Corp. Providence, RI (2009).